

1 **The effects of arbuscular mycorrhizal fungi (AMF) and *Rhizophagus irregularis***
2 **on soil microorganisms assessed by metatranscriptomics and metaproteomics**

3 Lammel, D.R.^{1,2}, Meierhofer, D.³, Johnston, P.^{1,4}, Mbedi, S.^{2,5}, Rillig, M.C.^{1,2}

4

5 ¹ Freie Universität Berlin, Institut für Biologie, D-14195 Berlin, Germany

6 ² Berlin-Brandenburg Institute of Advanced Biodiversity Research (BBIB), D-14195 Berlin, Ge

7 ³ Max Planck Institute for Molecular Genetics, D-14195 Berlin, Germany

8 ⁴ Berlin Center for Genomics in Biodiversity Research (BeGenDiv), D-14195 Berlin, Germany

9 ⁵ Museum für Naturkunde, D-10115 Berlin, Germany

10

11 Running title: **AMF select and activate soil microorganisms in the hyphosphere**

12

13 **Abstract**

14 Arbuscular mycorrhizal fungi (AMF) form symbioses with approximately 80% of plant
15 species and potentially benefit their hosts (e.g. nutrient acquisition) and the soil
16 environment (e.g. soil aggregation). AMF also affect soil microbiota and soil
17 multifunctionality. We manipulated AMF presence (via inoculation of non-sterile soil
18 with *Rhizophagus irregularis* and using a hyphal compartment design) and used
19 RNA-seq and metaproteomics to assess AMF roles in soil. The results indicated that
20 AMF drove an active soil microbial community expressing transcripts and proteins
21 related to nine metabolic functions, including the metabolism of C and N. We suggest
22 two possible mechanisms: 1) the AMF hyphae produce exudates that select a
23 beneficial community, or, 2) the hyphae compete with other soil microbes for
24 available nutrients and consequently induce the community to mineralize nutrients
25 from soil organic matter. We also identified candidate proteins that are potentially
26 related to soil aggregation, such as Lpt and HSP60. Our results bridge microbial
27 ecology and ecosystem functioning. We show that the AMF hyphosphere contains an
28 active community related to soil respiration and nutrient cycling, thus potentially

29 improving nutrient mineralization from soil organic matter and nutrient supply to the
30 plants.

31 **1. Introduction**

32 Recent studies indicated that plant roots select beneficial microbial
33 communities related to nutrient cycling in the rhizosphere (Mendes et al., 2014,
34 2018b; Baltrus, 2017; Yan et al., 2017; Schmidt et al., 2019). Therefore, we
35 hypothesized that arbuscular mycorrhizal fungi (AMF) also select beneficial microbial
36 communities in their hyphosphere (the volume of soil influenced by AMF hyphae).

37 Previous studies have found that AMF affect the soil microbial community
38 structure at the taxonomic level (Turrini et al., 2018; Xu et al., 2018; Bhatt et al.,
39 2019). However, even though such diversity studies based on ribosomal DNA
40 regions (e.g. 16/18S rRNA or ITS) are robust methods to assess microbial
41 community structure, they usually fail to correlate to environmental processes (Hall et
42 al., 2018; Lammel et al., 2018; Zhang et al., 2019). More accurate information related
43 to ecosystem functioning, interactions and nutrient cycling can be obtained by
44 assessing directly the metabolically active microbial community by RNA-seq and
45 proteomics (Mendes et al., 2018a; Yao et al., 2018). Thus, learning about the
46 metabolically active microbial community can be particularly important for a better
47 understanding of arbuscular mycorrhizal fungi (AMF) interactions with the soil
48 microbiota.

49 AMF are soil fungi that form a symbiosis with approximately 80% of plant
50 species. During the symbiosis, plant roots supply these fungi with carbohydrates and
51 fatty acids, while the fungi induce metabolic changes in the plant (including improved
52 plant growth and better plant response to biotic and abiotic stress) (Kameoka et al.;
53 Delavaux et al., 2017; Powell and Rillig, 2018; Begum et al., 2019; Mateus et al.,

54 2019). In addition to intimately associating with the plant root, the fungi also grow in
55 the soil, foraging for mineral nutrients and water, and affecting soil properties
56 (Kameoka et al.; Rillig and Mummey, 2006; Pepe et al., 2017). Consequently, AMF
57 have three main roles in soil, they: 1) taking up mineral nutrients and water, therefore
58 changing soil nutrient and water dynamics; 2) interacting with and changing soil
59 microbial communities, and 3) interacting with and modifying soil structure, e.g. by
60 aggregating soil (Rillig and Mummey, 2006; Cavagnaro et al., 2015; Powell and
61 Rillig, 2018; Bhatt et al., 2019).

62 Thus, it is not only relevant to understand how AMF change the dynamics of
63 nutrients in the soil but also how AMF induce changes in the soil microbial
64 community itself (Turrini et al., 2018; Bhatt et al., 2019). The inoculation of AMF,
65 remarkably *R. irregularis*, affects soil microbial community structure at the taxonomic
66 level (Changey et al., 2019). Moreover, some bacterial taxa are likely associated with
67 AMF spores, for example, *Proteobacteria* and *Firmicutes* (Battini et al., 2016;
68 Changey et al., 2019). However, detailed information about the effects of AMF on the
69 functionally active microbial community is still unavailable.

70 AMF also affect soil structure and their presence and abundance in soil is
71 typically correlated with soil aggregation (Rillig and Mummey, 2006; Schlüter et al.,
72 2019, 2019). On the other hand, soil aggregation affects microbial communities in
73 soil (Rillig et al., 2017; Upton et al., 2019). Soil aggregation is likely influenced by
74 direct effects of the AMF, such as hyphal enmeshment of soil particles and
75 production of exo-polymeric substances (EPS), and indirect effects, such as AMF
76 effects on microbial communities and the soil food web that could then change the
77 soil structure and aggregates (Rillig and Mummey, 2006). EPS can also be produced
78 by the microbial community, and include mainly polysaccharides and

79 lipopolysaccharides, which are synthesized by proteins such as Wza, Wca, Kps, Alg,
80 and Sac, and have been reported to be potentially correlated to soil aggregation
81 (Cania et al., 2019).

82 Another possible mechanism for soil aggregation could be that specific AMF
83 proteins may act as binding agents for soil particles. In the 1990's, a monoclonal
84 antibody was produced (MAb32B11) for the purpose of quantifying *R. irregularis* in
85 soil and the protein attached to that antibody was called "glomalin" (name derived
86 from *Glomus*) and it correlated with soil aggregation (Wright et al., 1996). Later,
87 general "glomalin related soil protein" ("GRSP") extractions methods were proposed,
88 but such methods were not specific and very likely biased by substances other than
89 glomalin (Rosier et al., 2006; Gillespie et al., 2011). Thus, the initial hypotheses
90 linking specific AMF proteins and soil aggregation are not confirmed. Gadkar and
91 Rillig (2006) provided initial evidence that the protein that attaches to the *R.*
92 *irregularis* 90's antibody (that was first called glomalin) may be a HSP60 protein.
93 HSP60 proteins (GroEL) are mainly molecular chaperons, but they can also have
94 moonlight functions, and are widespread proteins present in all living organisms
95 (Henderson et al., 2013). It is still unclear whether this protein can directly interact
96 with soil particles, but a priority research question is to quantify the abundance of
97 HSP60 from *R. irregularis* in soil compared to the natural occurrence of HSP60 from
98 the overall soil microbial community.

99 The objective of this study was to use RNA-seq and proteomics to investigate
100 the hypothesis that the AMF hyphosphere selects for a beneficial microbial
101 community. We mainly investigated the AMF effects on: 1) the C, N and P soil
102 community metabolism at the gene/protein level; 2) the soil microbial community
103 structure itself (assessed by the taxonomic affiliation of the genes/proteins); and 3)

104 transcripts and proteins potentially related to soil aggregation (such as the above-
105 mentioned proteins Wza, Wca, Kps, Alg, Sac and HSP60).

106

107 **2. Material and Methods**

108

109 *Compartmentalized experimental setup with hyphal compartment*

110 To test the effects of AMF on soil, we used the hyphal compartment approach
111 (Johnson et al., 2001; Leifheit et al., 2014). We established two main treatments,
112 non-sterile soil control and the same soil inoculated with *R. irregularis* (DAOM
113 197198) with ten replicates (ten pots) for each treatment. In all pots we placed the
114 hyphal compartment cores, and then the control soils were further divided into two
115 treatments: static cores and cores that were rotated three times per week. The
116 rotation of the cores severs fungal hyphae thus avoiding the growth of AMF inside
117 the rotated cores (Leifheit et al., 2014). So the experiment was finally divided into
118 three operational treatments: control with static cores (C), control with rotated cores
119 (rC) and static cores in soil inoculated with the AMF *R. irregularis* (A). Due to
120 technical limitations of advanced molecular techniques (e.g. sequencing costs), we
121 randomly chose four samples of each treatment for RNA-seq and five samples of
122 each treatment for proteomics. We report all the non-molecular analysis results for all
123 the treatments and replicates in Supplementary Material 1.

124 The soil used in the experiment was collected at the agricultural experimental
125 station of the Humboldt University in Dahlem (Berlin, Germany). The top soil from a
126 meadow (0-30 cm) was taken and air-dried at room temperature. The soil was an
127 Albic Luvisol (World Reference Base for soil resources, 1998) and had the following
128 physical-chemical characteristics: 73.6% sand, 18.8% silt, 7.6% clay; pH 7.1 (CaCl₂)

129 (analyses conducted by LUFA Rostock Agricultural Analysis and Research Institute,
130 Germany); 1.87% C (total) and a C/N ratio 15.6 (analyzed on an Euro EA C/N
131 analyzer, HEKAtech GmbH, Wegberg, Germany) (Rillig et al., 2010). The soil was
132 sieved to 4mm and root and plant material removed. Twenty plastic pots (20cm
133 diameter x 20cm high) were filled with five liters of this soil and core compartments
134 inserted in each pot (details about the cores in Leifheit et al., 2014).

135 Seeds of clover (*Trifolium repens* L) were surface sterilized with 70% ethanol
136 for 30 secs, followed by 3% sodium hypochlorite for 5 min, and then rinsed five times
137 with autoclaved water. Ten of these seeds were sown evenly in each pot, but after
138 germination only five plants were kept per pot. Half of the pots (ten) received the
139 main treatment and were inoculated with *R. irregularis* and the other half, ten pots,
140 were kept as control without inoculation. The inoculum was prepared from *R.*
141 *irregularis* that was grown under *in vitro* culture conditions (Rillig et al., 2010). A piece
142 of solid media containing hyphae and spores (“a loopful”) from the hyphae
143 compartment (containing 20 ± 7 spores) was inoculated nearby each seed in the
144 inoculated treatments and a “loopful” of sterile media was added nearby each seed
145 for the controls. The plants were grown in a greenhouse (22°C/ 18°C, day/ night) and
146 a photoperiod of 14h (a mix of natural light and supplementation of artificial light
147 when needed). An automatic irrigation system watered each pot with deionized water
148 once a day. It was programmed for 50ml/day for young plants and achieving 100
149 ml/day for larger plants. We fertilized the pots on days 15, 45 and 75 with 100 ml
150 Hoagland solution without P and N. On the same days we added 2 ml of full
151 Hoagland solution into the core compartments aiming to stimulate hyphal foraging
152 and growth into the cores.

153

154 *Experiment harvest*

155 After 105 days, the experiment was harvested. Pots were harvested one at a
156 time, to avoid delays in freezing the samples for molecular analysis. First, the shoots
157 of the plants were cut and placed in paper bags for later drying and biomass
158 determination. Then, 5 mm of the surface soil of the hyphal compartment cores were
159 removed (to avoid contamination from the surface) and the soil of each core was
160 transferred to a sterile 50ml conical tube and gently homogenized for 30s. From
161 these samples, two aliquots of 2ml soil were transferred to two sterile centrifuge
162 tubes and immediately frozen in liquid N₂ (to be later used in RNA extraction) and
163 5ml of soil transferred to a 5ml sterile centrifuge tube and frozen (to be later used for
164 protein extraction). All the spatulas and spoons were treated with 70% ethanol and
165 flamed between samples, and the plastic materials were previously autoclaved. The
166 samples were stored at -80°C. The remaining soil was air-dried for 48h at 40°C and
167 used for the soil aggregation and hyphal length analyses.

168

169 *Plant and soil analyses*

170 Plant shoots were dried in an oven for 48h at 60°C and then weighed. We
171 analyzed soil aggregation by measuring the newly formed aggregates and water
172 stable aggregates (WSA), and we also analyzed AMF and non-AMF hyphal length in
173 the soil.

174 The newly formed aggregates were measured by weighing the dry soil
175 particles >2mm and dividing this value by the total weight of the soil sample. For the
176 WSA measurement we used a wet sieving apparatus (Kemper and Rosenau, 1986).
177 The method was slightly modified as described by Leifheit et al. (2014): 4.0 g of dried
178 soil were rewetted by capillary action and sieved for 3 min using a 250 µm sieve. The

179 coarse matter was separated by crushing the aggregates that remained on the sieve
180 and the small particles washed out through the sieve. Coarse matter and soil were
181 dried at 60°C for 48 h and WSA calculated and corrected for coarse matter.

182 Hyphal length was determined by extraction from 4.0 g of soil, staining with
183 Trypan blue and followed by microscopy (Jakobsen et al., 1992; Rillig et al. 1999).
184 Dark to light blue stained aseptate hyphae with characteristic unilateral angular
185 projections (“elbows and coils”) were considered mycorrhizal (Mosse, 1959), whereas
186 non-blue stained or blue stained hyphae with regular septation or straight growth
187 were considered non-mycorrhizal (Leifheit et al., 2014). We also counted the number
188 of AMF spores on the slides (Supp. Material 1).

189

190 *RNA extraction and sequencing*

191 RNA was extracted from 2g of the frozen soil using the RNeasy PowerSoil
192 Total RNA Kit (Qiagen, Germany). Since an important goal of RNA-seq was to
193 produce a broad and annotated library to allow protein identification, we adopted two
194 library strategies for mRNA enrichment. First, we targeted eukaryotic mRNA
195 enrichment in the samples and used 60% of the volume of each RNA extract for poly-
196 A enrichment using the kit NEXTflex Poly(A) Beads (Perkin Elmer, USA). Secondly,
197 we targeted the transcripts from the full soil diversity using rRNA depletion by
198 hybridization. For that, the four replicates of each treatment were combined in pairs,
199 using 20% of the volume of the RNA extracts from each sample, yielding two
200 samples for each treatment (we pooled samples to increase sequencing depth). The
201 samples were then treated with the kit RiboMinus Bacteria following the
202 manufacturer’s instructions (ThermoFischer, USA).

203 The 18 mRNA samples, 12 samples poly-A enriched and six samples rRNA
204 depleted, were prepared for sequencing using NextFlex Rapid Directional RNA
205 SeqKit (Perkin Elmer, USA). All the samples were evaluated in an Agilent
206 TapeStation and quantified by QuBit (Invitrogen, USA). The samples of each library
207 were pooled in equimolar ratios for each library strategy. The libraries were then
208 pooled together using a six-fold higher concentration of the rRNA depletion library
209 compared to the poly-A library (since we expected higher diversity for the first). The
210 libraries were sent for sequencing to a commercial company using the Illumina HiSeq
211 X Ten platform. The sequences were deposited at the GenBank server
212 (<https://www.ncbi.nlm.nih.gov/genbank> - Bioproject number PRJNAxxxxx).

213

214 *Soil RNA-seq analysis*

215 The sequences from the HiSeq run were quality checked and demultiplexed
216 using the bcl2fastq software (Illumina, USA). All the sequences were then processed
217 together using the software Trinity and assembled and cleaned of rRNA (Grabherr et
218 al., 2011). The assemblage was annotated by Blast2go (Götz et al., 2008). The
219 sequences were also further classified according to the SEED system from MG-
220 RAST (Wilke et al., 2016). Lastly, the reads of each sample were mapped to the
221 sequences assembled by the software Trinity or to the genome of *R. irregularis* DAO
222 JGI v2 using the software Salmon (Grabherr et al., 2011; Morin et al., 2019). The
223 annotation table and the counting table of the mapped reads were further exported
224 for analysis in R.

225

226 *Metaproteomics*

227 Protein extraction was performed based on five grams of frozen soil for all
228 three conditions in biological quintuplicates by the addition of extraction buffer
229 containing 100 mM Tris-HCl pH 8.0, 5% w/v sodium dodecyl sulphate, and 10 mM
230 dithiothreitol. Samples were vortexed and boiled for 10 min at 100°C, centrifuged at
231 4,000 x g for 10 min and the supernatants were transferred into new protein low-
232 binding tubes. Proteins were then precipitated by the addition of chilled trichloroacetic
233 acid to a final concentration of 20% and kept at -80°C overnight. Proteins were
234 pelleted at 4,000 x g for 30 min, washed twice with cold acetone (-20°C), and air-
235 dried, as described in (Qian and Hettich, 2017).

236 Protein extracts were reduced and alkylated under denaturing conditions by
237 the addition of 200 µL of a buffer containing 3 M guanidiniumhydrochlorid, 10 mM tris(2-
238 carboxyethyl)phosphine (TCEP), 40 mM chloroacetamide (CAA), and 100 mM Tris
239 pH 8.5 to prevent proteolytic activities, briefly vortexed and boiled for 10 min at 95°C
240 at 1000 rpm. Pellet disintegration was achieved by a sonicator with five cycles of
241 P150W, C60%, A100% (Hielscher, Teltow, Germany). After centrifugation at 15,000
242 rcf at 4°C for 10 min, supernatants were transferred into new protein low binding
243 tubes. The lysates were loaded into the preOmics in-stage tip kit cartridges (iST kit
244 96x, Martinsried, Germany) to remove humics, centrifuged at 3,800 rcf for 3 min,
245 washed with 8 M urea by pipetting up and down ten times and centrifuged again. The
246 lysates were digested and purified according to the preOmics in-stage tip kit
247 (preOmics). In brief, 50 µl lysis buffer was added, diluted with resuspension buffer
248 and digested after 10 min at 37°C at 500 rpm overnight. After several washing steps,
249 peptides were eluted sequentially in three fractions using the SDB-RPS-1 and -2
250 buffers (Kulak et al., 2014) and the elution buffer provided by preOmics. Eluates were
251 first dried in a SpeedVac, then dissolved in 5% acetonitrile and 2% formic acid in

252 water, briefly vortexed, and sonicated in a water bath for 30 seconds for subsequent
253 analysis on a nanoLC-MS/MS.

254

255 *LC-MS instrument settings for shotgun proteome profiling and data analysis*

256 LC-MS/MS was carried out by nanoflow reverse-phase liquid chromatography
257 (Dionex Ultimate 3000, Thermo Scientific, Waltham, MA) coupled online to a Q-
258 Exactive HF Orbitrap mass spectrometer (Thermo Scientific). The LC separation was
259 performed using a PicoFrit analytical column (75 μm ID \times 50 cm long, 15 μm Tip ID
260 (New Objectives, Woburn, MA) in-house packed with 3- μm C18 resin (Reprosil-AQ
261 Pur, Dr. Maisch, Ammerbuch-Entringen, Germany). Peptides were eluted using a
262 gradient from 3.8 to 50 % solvent B in solvent A over 121 min at 266 nL per minute
263 flow rate. Solvent A was 0.1 % formic acid and solvent B was 79.9 % acetonitrile, 20
264 % water, 0.1 % formic acid. An electrospray was generated by applying 3.5 kV. A
265 cycle of one full Fourier transformation scan mass spectrum (300–1750 m/z,
266 resolution of 60,000 at m/z 200, AGC target 1e^6) was followed by 12 data-dependent
267 MS/MS scans (resolution of 30,000, AGC target 5e^5) with a normalized collision
268 energy of 25 eV. In order to avoid repeated sequencing of the same peptides a
269 dynamic exclusion window of 30 sec. was used. In addition, only the peptide charge
270 states between two to eight were sequenced.

271

272 *Label-Free Proteomics Data Analysis*

273 Raw MS data were processed with MaxQuant software (v1.6.0.1) and
274 searched against the *Rhizophagus irregularis* UP000236242_747089 database,
275 released in May/2019, or the annotated RNA-seq assemblage. A false discovery rate
276 (FDR) of 0.01 for proteins and peptides, a minimum peptide length of 7 amino acids,

277 a precursor mass tolerance to 20 ppm for the first search and 4.5 ppm for the main
278 search were required. A maximum of two missed cleavages was allowed for the
279 tryptic digest. Cysteine carbamidomethylation was set as fixed modification, while N-
280 terminal acetylation and methionine oxidation were set as variable modifications.

281 The tables generated by MaxQuant were further processed using the online
282 server ANPELA (“analysis and performance assessment of label-free
283 metaproteomes”), data were log transformed and processed by the online pipeline,
284 including missing data imputation by the K-nearest Neighbor algorithm (KNN) and
285 mean normalization (MEA) (Tang et al., 2019).

286

287 *Statistical analysis*

288 Analyses were performed in R version 3.5. Plant biomass, water stable
289 aggregates and hyphal length were analyzed by ANOVA, followed by the Tukey
290 posthoc test. We also correlated variables using Spearman’s rank correlation
291 coefficient (ρ). The distribution of the data and effect sizes were analyzed by the R-
292 DBR package (SI Figure S1).

293 The tables previously obtained from the RNA-seq and proteomics were
294 aggregated with the SEED functions for a first explanatory analysis. Differences
295 between the samples were analyzed by cluster analysis. The taxonomy obtained by
296 the Blast2go annotation was used in the diversity analysis and RDA using R-Vegan.
297 The data were further analyzed by R packages DeSeq2/Alx2 and the online server
298 GMine (<http://cgenome.net/gmine>) (Quinn et al., 2018). Since both RNA-seq data
299 sets were analyzed according to the pool of identified sequences, we treated them as
300 compositional data, considering the centered log-ratio of the values of each
301 gene/protein for each sample (Gloor et al., 2017). We report the log-ratio fold change

302 of the gene/proteins and Welch's t-test with Benjamini-Hochberg corrected statistical
303 probabilities, calculated by the R-packages DeSeq2 and Alx2 or the online server
304 Gmine.

305

306 **3. Results**

307 We evaluated the effects of *R. irregularis* inoculation compared to control soil.
308 Plants were harvested at 105 days, but no difference was observed in the shoot plant
309 biomass (Figure 1 A-B and SI S1).

310 We further evaluated the soil compartments that were divided in three
311 treatments with five replicates each: 1) control with static cores (C), 2) control with
312 rotated cores (rC) and 3) cores of soil inoculated with the AMF *R. irregularis* (A).
313 First, we detected that the C and A cores were colonized by AMF, while very few
314 AMF hyphae were observed in the rC (Figure 1.C). We also detected colonization by
315 non-AMF hyphae in all the cores, but there was no difference ($P=0.356$) among
316 treatments (Figure 1 D). Secondly, we detected increases in soil aggregation. At the
317 beginning of the experiment, all soil was sieved to 2 mm and we observed at the
318 harvest time 57 ± 4 % new formed aggregates, however no strong differences were
319 observed across treatments ($P=0.121$). We also observed increases in WSA during
320 the experiment, from $46 \% \pm 3$ at the beginning, increased to 56-61 % after 105 days
321 (Figure 1.E.). At 105 days we found higher soil aggregation in the cores inoculated
322 with *R. irregularis* in relation to the rotated cores ($P=0.036$) (Figure 1.D-E). We also
323 detected a correlation between AMF hyphal length and WSA across the treatments
324 ($\rho=0.67$, $P<0.01$), as also between non-AMF hyphae and WSA ($\rho=0.60$, $P<0.01$).

325

326 *Effects of AMF on soil community metabolism*

327 The samples were further analyzed in terms of metatranscriptomics (Figures
328 2-4). The HiSeq sequencing run yielded 180 million reads (SI Figure S2). From that,
329 for the rRNA depletion libraries we recovered an average of 6 million reads for the C
330 treatment, 2.5 million for rC and 6.5 million for A. For the poly-A libraries we
331 recovered an average of 21.5 million reads for the C treatment, 30 million for rC and
332 25 million for A. For the Poly-A enrichment library, around of 50% of the transcripts
333 were still from bacteria (Figure 4). This indicates that Poly-A selection from soil is
334 challenging, since most of the transcripts in soils are generally from bacteria (Mendes
335 et al., 2018a; Schlüter et al., 2019). The method could be improved in future by, for
336 example, by repeating the poly-A selection for several times. Based on the Blast2go
337 annotation, from the poly-A library, we were able to recover around 0.47% of reads of
338 AMF (*Glomeromycota*) for C, 0.36% for rC and 0.46% for A (SI Figure S2). For the
339 rRNA depletion library we were able to recover 0.45% AMF reads for C, 0.32% reads
340 for rC and 0.42% for A.

341 The transcript analyses indicated several differences in gene expression
342 related to C, N, P and respiration processes clustered by the MG-RAST SEED terms
343 (Figure 2-3). From the 616,863 genes assembled by Trinity, 161,702 could be
344 annotated to the 29 SEED categories “level 1”. We further segregated the
345 “GroEL/HSP60” category (SEED level 2) from the category “protein” in SEED level 1,
346 to better test our third hypothesis about HSP60. The first exploratory analysis, the
347 heat map and cluster analysis, indicated that the samples were distinctly clustered
348 between the rotated core and the other treatments with high abundance of AMF
349 hyphae (Figure 2.A). Some clustering was observed differentiating the static core
350 control and the *R. irregularis* treatment (Figure 2.A). Notice that the heat map scale is
351 not about negative or positive gene expression, but it is based on the scaled

352 centered log-ratio (CLR) transformation recommended for compositional data and
353 reflects the relative abundance of each metabolic category in each sample. From the
354 29 functional categories, 15 categories were associated by a network analysis to the
355 presence of AMF hyphae in soil (Figure 3). The analyses indicated that *R. irregularis*
356 inoculation had increased expression of genes related to RNA metabolism,
357 respiration and GroEL/HSP60. The control sample, that also had AMF hyphae, had
358 intermediate values between the inoculated and the rotated core treatments and was
359 related with C, N, P and S metabolism. The rotated control was related mostly with
360 cell division, mobility, fatty acids, and secondary metabolism (Figure 3). We found a
361 correlation between AMF hyphal length and transcripts related to respiration ($r=0.66$,
362 $P=0.028$), but no strong evidence for a correlation between hyphal length and total
363 GroEL/HSP60 transcripts ($r=0.47$, $P=0.14$).

364 For the proteomic data, we identified 1336 proteins using the RNA-seq as
365 reference, and the data normalized by ANPELA indicated a strong separation of the
366 samples by treatment (SI Figure S3), and a volcano plot identified 103 proteins that
367 were more abundant in C and A than in the rotated cores (Supp. Figure 3). From all
368 the proteins, 398 were identified at MG-RAST SEED categories (Figure 2.B), and,
369 again, there was a differentiation between rotate cores to the control and soil
370 inoculated with *R. irregularis*. Considering these 398 proteins, there was a decrease
371 in 19 SEED categories in the rotated cores (Figure 3.B) and thus the network
372 analyses were strongly influenced by the non-rotated treatments, that can be
373 observed by the color of the network nodes, indicating mainly the non-rotated
374 treatments (Figure 3.D). GroEL/HSP60 was more abundant in the soil cores
375 inoculated with *R. irregularis*. Using the *R. irregularis* genome as reference, we

376 identified 51 proteins and most of them were proteins related to protein metabolism,
377 including heat shock proteins (we report on this separately in the section about HSP).
378

379 *Effects of AMF on soil community structure*

380 The metatranscriptomic data were then analyzed taxonomically. From the
381 616,863 genes assembled by Trinity, 199,566 were annotated by Blast2go. All the
382 samples were dominated by Bacteria (Figure 4). The rRNA depletion library had
383 approx. 45% of Bacteria for the A and C treatments and approx. 65% in the rC
384 (Figure 4.A). For the poly-A libraries, it was also approx. 45% of Bacteria for the A
385 and C treatments, but approx. 50% of *Bacteria* in the rC. The microbial community
386 structure was further investigated by RDA (Figures 4. C1 and D1). For both, *Bacteria*
387 and *Eukaryota*, the samples were better clustered by the libraries made from the
388 mRNA enrichment by rRNA depletion libraries (“m” code in the figures). For the
389 depletion libraries, the rotated cores had a distinct community structure when
390 compared to the static-control soil and the soil inoculated with *R. irregularis*
391 (perMANOVA, $P < 0.001$ for both, *Bacteria* and *Eukaryota*). However, clustering of the
392 samples from the poly-A libraries was not strongly supported (perMANOVA, $P < 0.12$
393 for *Bacteria* and $P < 0.20$ for *Eukaryota*).

394 The samples were further analyzed in detail in terms of the composition of
395 *Bacteria* and *Eukaryota* sequences. The RNA-seq data indicated that all the samples
396 were dominated by *Actinobacteria* and *Proteobacteria* (no difference among
397 treatments was observed; $P = 0.2$), but a reduction of *Firmicutes* (Aldex2, $P = 0.052$)
398 was observed in the rotated cores (Figure 4.C2). Considering *Eukaryota*, the
399 samples were dominated by *Longamoebia*, *Protosteliales* and *Streptophyta* (Figure

400 4. D2). *Fungi* accounted for around 15% of the *Eukaryota* reads, and *Glomeromycota*
401 for around 0.4% of the reads (SI Figure S2).

402

403 *Effects of AMF on transcripts/proteins potentially linked to soil aggregation*

404 We screened for genes/proteins potentially related to soil aggregation. We
405 explored a list of genes/proteins including genes related to EPS metabolism (Cania
406 et al., 2019), such as polysaccharide export outer membrane (Wza), capsular
407 polysaccharide export system (Kps) and lipopolysaccharide export proteins (Lpt). We
408 did not find differences for most of the genes/proteins, but found in the
409 metatranscriptome that Lpt (Figure 5A) was more abundant in rotated core samples
410 (z-score 0.6-0.9), when compared to the control and *R. irregularis* inoculated
411 treatments ($P < 0.001$).

412 We further evaluated HSP60/GroEL, which was very abundant across all
413 treatments, especially in the cores with higher abundance of AMF hyphae (Figure 2).
414 In all treatments, at the RNA level, HSP60/GroEL was predominantly of bacterial
415 origin, particularly from *Acidobacteria* and *Proteobacteria* (SI Figure S5 A1-2). Of the
416 few reads of eukaryotic origin, the great majority was from *Basidiomycota*, with the
417 exception of the rotated cores, which had a high abundance of reads from
418 *Longamoebia* (SI Figure S5 A3). In the proteome, the vast majority of identified
419 HSP60/GroEL proteins came from *Bacteria* (app. 99% across all treatments), and
420 they were predominantly from *Acidobacteria* and *Proteobacteria* (SI Figure S5 B).

421 We found a correlation between the total HSP60/GroEL with the AMF hyphal
422 length for the total metaproteome ($r = 0.57$, $P = 0.026$), but little evidence for the total
423 metatranscriptome ($r = 0.47$, $P = 0.14$). However, as described before, most of these

424 HSP60/GroEL came from *Bacteria* (SI Figure S5 A1). We observed no correlation
425 between total HSP60/GroEL and WSA (all had $P>0.2$).

426 We further looked at the proteins identified from *R. irregularis* in the
427 metaproteome and there were no differences in HSP60/GroEL ($P=0.21$) across the
428 treatments (Figure 6). We compared this result with tubulins (Alfa+Beta) ($P=0.08$),
429 which are essential proteins related to fungal growth, and observed a very similar MS
430 signal intensity to the HSP60/GroEL protein. We screened the other HSPs from *R.*
431 *irregularis* and detected also little evidence for differences across treatments for two
432 other HSP, the HSP70 (Uniprot A0A2H5SZG6, $P=0.14$) and HSP70 (Uniprot
433 U9SYW5, $P=0.07$). None of these proteins were correlated with AMF hyphal length
434 or WSA (all had $P>0.2$). These results also indicated that *R. irregularis* transcripts
435 and proteins were a small proportion of the full microbial community (we estimated
436 AMF being between 0.3-0.5% of the active community, SI Figure S1).

437

438 **4. Discussion**

439

440 In this study, we investigated the effects of AMF on soil microbial communities
441 using soil RNA-seq and metaproteomics. We detected that AMF drove the active
442 microbial community as well as transcripts and proteins related to metabolic
443 functions. First, we showed that the presence of AMF induced changes in transcripts
444 and proteins in soil related to several metabolic processes, including protein
445 metabolism (N cycle) and respiration (C cycle). Secondly, we showed that *R.*
446 *irregularis* induces changes in the soil microbial community, which was largely
447 dominated by *Bacteria*. And thirdly, we detected transcripts and proteins that could
448 be related to soil aggregation.

449 Previous knowledge about AMF affecting soil functions was obtained mostly
450 by inoculation studies, or by quantifying AMF hyphae in soils and correlating them
451 with specific functions, such as nitrogen uptake or soil aggregation (Powell and Rillig,
452 2018; Hestrin et al., 2019; Rillig et al., 2019). To the best of our knowledge, this was
453 the first attempt to experimentally assess metatranscriptomes and metaproteomes to
454 estimate the contribution of AMF to the metabolism of the entire soil community. We
455 find that only 0.3-0.5% of the transcripts/proteins were of AMF origin and our data
456 indicate that AMF induced significant shifts in soil community metabolism when
457 compared to the rotated core control (Figures 2 and 3).

458 Our results bridge between microbial ecology and ecosystems functioning.
459 The data suggest that the AMF hyphosphere drive an active community related to
460 soil respiration and nutrient cycling, potentially improving nutrient mineralization from
461 soil organic matter and nutrient supply to plants. Previous studies also presented
462 several lines of evidence that AMF influence the microbial community and that these
463 fungi are important players in the carbon cycle, P and N dynamics and soil
464 respiration (Nottingham et al., 2010; Zhang et al., 2016; Powell and Rillig, 2018;
465 Hestrin et al., 2019). Interestingly, previous studies have suggested that AMF are
466 associated with specific bacterial communities and that these communities have
467 complementary functional roles to the AMF (Battini et al., 2016; Turrini et al., 2018).
468 Our data corroborate these findings in a general way, since the community had
469 increased expression of genes/proteins related to general soil processes in the
470 presence of the AMF hyphae (Figures 2 and 3).

471 Thus, we present evidence that arbuscular mycorrhizal fungi (AMF) select for
472 beneficial microbial communities in their hyphosphere. We suggest two possible
473 mechanisms to be tested in future: 1) the AMF hyphae produce exudates that select

474 a beneficial microbial community, analogous to reports for plant roots (Baltrus, 2017);
475 or, 2) AMF hyphae compete with the microbial community for available nutrients and
476 consequently induce the community to mineralize nutrients from soil organic matter
477 (Hestrin et al., 2019).

478 Moreover, our study showed that the soil communities were dominated by
479 transcripts and proteins of bacterial origin (Figure 4). We observed that the samples
480 were dominated by *Proteobacteria* and had an increased relative abundance of
481 *Firmicutes* in the hyphal compartments, and both groups were previously reported to
482 be predominantly associated with AMF (Battini et al., 2016; Turrini et al., 2018).
483 Interestingly in the rotated cores there was an increased expression of bacterial *lpt*
484 genes (lipopolysaccharide export proteins). These genes can be related to soil
485 aggregation and we speculate that these could be related to soil aggregation in the
486 rotated cores, since soil aggregates increased from the beginning of the experiment
487 to the harvest (Cania et al., 2019).

488 Lastly, our data showed a high abundance and diversity of HSP60 (GroEL)
489 across the soil samples detected by RNA-seq and by proteomics. This can be
490 explained in two ways; first, this chaperon occurs across all living organisms and it
491 has essential functions in protein folding and cell metabolism, in addition to moonlight
492 functions (Henderson et al., 2013). Second, for the proteome samples, our method
493 included the boiling of samples and this can likely select for thermostable proteins,
494 such as HSPs (Rosier et al., 2006; Gillespie et al., 2011). Furthermore, HSP60
495 abundance may not only reflect cell abundance, but also the metabolic status of cells
496 (Henderson et al., 2013). Moreover, our data clearly showed the high complexity of a
497 soil community sample and that HSP60 is highly abundant and diverse in soil. We
498 also observed that at nucleotide level the HSP from *R. irregularis* are divergent

499 enough to be differentiated from the community sequences (Magurno et al., 2019),
500 but due codon redundancy they are highly conserved at the amino acid level. This
501 implies that during processing for proteomics the HSP60 could potentially be cleaved
502 in positions to overlap MS peptides spectra of HSP60/GroEL from other members of
503 the microbial community, and theoretically causing noise in the quantification of
504 HSP60 from AMF. Previous studies using the monoclonal antibody MAb32B11 for *R.*
505 *irregularis* already showed that HSP60 quantifications in soil are also difficult due to
506 the complex composition of organic material in soil and could make quantifications
507 imprecise (Rosier et al., 2006). Our new findings also bring additional evidence to
508 avoid quantifying GRSPs as a proxy to quantify AMF proteins in soil (Rosier et al.,
509 2006; Gillespie et al., 2011). Nevertheless, we are optimistic that future works using
510 high-resolution proteomics, perhaps in simpler soil communities, will be able to
511 identify specific proteins from AMF in soil and potentially correlating them with
512 ecosystems functions, such as soil aggregation.

513

514 **5. Conclusions**

515

516 We provide evidence that the AMF hyphosphere drives an active community
517 related to soil respiration and nutrient cycling, potentially improving nutrient
518 mineralization from soil organic matter and nutrient supply to plants. Overall, our
519 results show that AMF have an intense effect on the soil microbial community and on
520 the metabolic pathways related to soil functions and nutrient dynamics. These
521 findings contribute to a better understanding of the role of AMF in soil and how they
522 drive soil metabolism and microbial community structure.

523

524 **6. Acknowledgments**

525

526 We acknowledge Alexander-von-Humboldt Foundation and CAPES Foundation for a
527 postdoctoral grant awarded to DRL, and Freie Universität Berlin and the Max Planck
528 Society for funding this work.

529

530 **7. References**

531

- 532 Baltrus, D. A. (2017). Adaptation, specialization, and coevolution within phytobiomes.
533 *Current Opinion in Plant Biology* 38, 109–116. doi:10.1016/j.pbi.2017.04.023.
- 534 Battini, F., Cristani, C., Giovannetti, M., and Agnolucci, M. (2016). Multifunctionality and
535 diversity of culturable bacterial communities strictly associated with spores of the
536 plant beneficial symbiont *Rhizophagus intraradices*. *Microbiological Research* 183,
537 68–79. doi:10.1016/j.micres.2015.11.012.
- 538 Begum, N., Qin, C., Ahanger, M. A., Raza, S., Khan, M. I., Ashraf, M., et al. (2019). Role of
539 Arbuscular Mycorrhizal Fungi in Plant Growth Regulation: Implications in Abiotic
540 Stress Tolerance. *Front. Plant Sci.* 10. doi:10.3389/fpls.2019.01068.
- 541 Bhatt, P., Joshi, D., Kumar, N., and Kumar, N. (2019). “Recent Trends to Study the
542 Functional Analysis of Mycorrhizosphere,” in *Mycorrhizosphere and Pedogenesis*,
543 eds. A. Varma and D. K. Choudhary (Singapore: Springer Singapore), 181–190.
544 doi:10.1007/978-981-13-6480-8_11.
- 545 Cania, B., Vestergaard, G., Kublik, S., Köhne, J. M., Fischer, T., Albert, A., et al. (2019).
546 Biological Soil Crusts from Different Soil Substrates Harbor Distinct Bacterial Groups
547 with the Potential to Produce Exopolysaccharides and Lipopolysaccharides. *Microb*
548 *Ecol.* doi:10.1007/s00248-019-01415-6.
- 549 Cavagnaro, T. R., Bender, S. F., Asghari, H. R., and Heijden, M. G. A. van der (2015). The
550 role of arbuscular mycorrhizas in reducing soil nutrient loss. *Trends in Plant Science*
551 20, 283–290. doi:10.1016/j.tplants.2015.03.004.
- 552 Changey, F., Meglouli, H., Fontaine, J., Magnin-Robert, M., Tisserant, B., Lerch, T. Z., et al.
553 (2019). Initial microbial status modulates mycorrhizal inoculation effect on
554 rhizosphere microbial communities. *Mycorrhiza*. doi:10.1007/s00572-019-00914-1.
- 555 Delavaux, C. S., Smith-Ramesh, L. M., and Kuebbing, S. E. (2017). Beyond nutrients: a
556 meta-analysis of the diverse effects of arbuscular mycorrhizal fungi on plants and
557 soils. *Ecology* 98, 2111–2119. doi:10.1002/ecy.1892.

- 558 Gadkar, V., and Rillig, M. C. (2006). The arbuscular mycorrhizal fungal protein glomalin is a
559 putative homolog of heat shock protein 60. *FEMS Microbiol Lett* 263, 93–101.
560 doi:10.1111/j.1574-6968.2006.00412.x.
- 561 Gillespie, A. W., Farrell, R. E., Walley, F. L., Ross, A. R. S., Leinweber, P., Eckhardt, K.-U.,
562 et al. (2011). Glomalin-related soil protein contains non-mycorrhizal-related heat-
563 stable proteins, lipids and humic materials. *Soil Biology and Biochemistry* 43, 766–
564 777. doi:10.1016/j.soilbio.2010.12.010.
- 565 Gloor, G. B., Macklaim, J. M., Pawlowsky-Glahn, V., and Egozcue, J. J. (2017). Microbiome
566 Datasets Are Compositional: And This Is Not Optional. *Front. Microbiol.* 8.
567 doi:10.3389/fmicb.2017.02224.
- 568 Götz, S., García-Gómez, J. M., Terol, J., Williams, T. D., Nagaraj, S. H., Nueda, M. J., et al.
569 (2008). High-throughput functional annotation and data mining with the Blast2GO
570 suite. *Nucleic Acids Res* 36, 3420–3435. doi:10.1093/nar/gkn176.
- 571 Grabherr, M. G., Haas, B. J., Yassour, M., Levin, J. Z., Thompson, D. A., Amit, I., et al.
572 (2011). Trinity: reconstructing a full-length transcriptome without a genome from
573 RNA-Seq data. *Nat Biotechnol* 29, 644–652. doi:10.1038/nbt.1883.
- 574 Henderson, B., Fares, M. A., and Lund, P. A. (2013). Chaperonin 60: a paradoxical,
575 evolutionarily conserved protein family with multiple moonlighting functions.
576 *Biological Reviews* 88, 955–987. doi:10.1111/brv.12037.
- 577 Hestrin, R., Hammer, E. C., Mueller, C. W., and Lehmann, J. (2019). Synergies between
578 mycorrhizal fungi and soil microbial communities increase plant nitrogen acquisition.
579 *Commun Biol* 2, 1–9. doi:10.1038/s42003-019-0481-8.
- 580 Kameoka, H., Maeda, T., Okuma, N., and Kawaguchi, M. Structure-Specific Regulation of
581 Nutrient Transport and Metabolism in Arbuscular Mycorrhizal Fungi. *Plant Cell*
582 *Physiol.* doi:10.1093/pcp/pcz122.
- 583 Lammel, D. R., Barth, G., Ovaskainen, O., Cruz, L. M., Zanatta, J. A., Ryo, M., et al. (2018).
584 Direct and indirect effects of a pH gradient bring insights into the mechanisms driving
585 prokaryotic community structures. *Microbiome* 6. doi:10.1186/s40168-018-0482-8.
- 586 Leifheit, E. F., Verbruggen, E., and Rillig, M. C. (2014). Rotation of hyphal in-growth cores
587 has no confounding effects on soil abiotic properties. *Soil Biology and Biochemistry*
588 79, 78–80. doi:10.1016/j.soilbio.2014.09.006.
- 589 Magurno, F., Malicka, M., Posta, K., Wozniak, G., Lumini, E., and Piotrowska-Seget, Z.
590 (2019). Glomalin gene as molecular marker for functional diversity of arbuscular
591 mycorrhizal fungi in soil. *Biol Fertil Soils* 55, 411–417. doi:10.1007/s00374-019-
592 01354-x.
- 593 Mateus ID, Masclaux FG, Aletti C, Rojas EC, Savary R, Dupuis C, et al. Dual RNA-seq
594 reveals large-scale non-conserved genotype × genotype-specific genetic reprogramming
595 and molecular crosstalk in the mycorrhizal symbiosis. *ISME J* 2019; **13**: 1226–1238.

- 596 Mendes, L. W., Kuramae, E. E., Navarrete, A. A., van Veen, J. A., and Tsai, S. M. (2014).
597 Taxonomical and functional microbial community selection in soybean rhizosphere.
598 *The ISME Journal* 8, 1577–1587. doi:10.1038/ismej.2014.17.
- 599 Mendes, L. W., Mendes, R., Raaijmakers, J. M., and Tsai, S. M. (2018a). Breeding for soil-
600 borne pathogen resistance impacts active rhizosphere microbiome of common bean.
601 *ISME J* 12, 3038–3042. doi:10.1038/s41396-018-0234-6.
- 602 Mendes, L. W., Raaijmakers, J. M., de Hollander, M., Mendes, R., and Tsai, S. M. (2018b).
603 Influence of resistance breeding in common bean on rhizosphere microbiome
604 composition and function. *ISME J* 12, 212–224. doi:10.1038/ismej.2017.158.
- 605 Morin, E., Miyauchi, S., Clemente, H. S., Chen, E. C. H., Pelin, A., Providencia, I. de la, et al.
606 (2019). Comparative genomics of *Rhizophagus irregularis*, *R. cerebriforme*, *R.*
607 *diaphanus* and *Gigaspora rosea* highlights specific genetic features in
608 Glomeromycotina. *New Phytologist* 222, 1584–1598. doi:10.1111/nph.15687.
- 609 Nottingham, A. T., Turner, B. L., Winter, K., Heijden, M. G. A. van der, and Tanner, E. V. J.
610 (2010). Arbuscular mycorrhizal mycelial respiration in a moist tropical forest. *New*
611 *Phytologist* 186, 957–967. doi:10.1111/j.1469-8137.2010.03226.x.
- 612 Pepe, A., Sbrana, C., Ferrol, N., and Giovannetti, M. (2017). An in vivo whole-plant
613 experimental system for the analysis of gene expression in extraradical mycorrhizal
614 mycelium. *Mycorrhiza* 27, 659–668. doi:10.1007/s00572-017-0779-7.
- 615 Powell, J. R., and Rillig, M. C. (2018). Biodiversity of arbuscular mycorrhizal fungi and
616 ecosystem function. *New Phytologist* 220, 1059–1075. doi:10.1111/nph.15119.
- 617 Qian, C., and Hettich, R. L. (2017). Optimized Extraction Method To Remove Humic Acid
618 Interferences from Soil Samples Prior to Microbial Proteome Measurements. *J.*
619 *Proteome Res.* 16, 2537–2546. doi:10.1021/acs.jproteome.7b00103.
- 620 Quinn, T. P., Crowley, T. M., and Richardson, M. F. (2018). Benchmarking differential
621 expression analysis tools for RNA-Seq: normalization-based vs. log-ratio
622 transformation-based methods. *BMC Bioinformatics* 19, 274. doi:10.1186/s12859-
623 018-2261-8.
- 624 Rillig, M. C., Aguilar-Trigueros, C. A., Camenzind, T., Cavagnaro, T. R., Degruene, F.,
625 Hohmann, P., et al. (2019). Why farmers should manage the arbuscular mycorrhizal
626 symbiosis. *New Phytologist* 222, 1171–1175. doi:10.1111/nph.15602.
- 627 Rillig, M. C., Mardatin, N. F., Leifheit, E. F., and Antunes, P. M. (2010). Mycelium of
628 arbuscular mycorrhizal fungi increases soil water repellency and is sufficient to
629 maintain water-stable soil aggregates. *Soil Biology and Biochemistry* 42, 1189–1191.
630 doi:10.1016/j.soilbio.2010.03.027.
- 631 Rillig, M. C., Muller, L. A., and Lehmann, A. (2017). Soil aggregates as massively concurrent
632 evolutionary incubators. *ISME J* 11, 1943–1948. doi:10.1038/ismej.2017.56.
- 633 Rillig, M. C., and Mummey, D. L. (2006). Mycorrhizas and soil structure. *New Phytologist*
634 171, 41–53. doi:10.1111/j.1469-8137.2006.01750.x.

- 635 Rosier, C. L., Hoyer, A. T., and Rillig, M. C. (2006). Glomalin-related soil protein:
636 Assessment of current detection and quantification tools. *Soil Biology and*
637 *Biochemistry* 38, 2205–2211. doi:10.1016/j.soilbio.2006.01.021.
- 638 Schlüter, S., Eickhorst, T., and Mueller, C. W. (2019). Correlative Imaging Reveals Holistic
639 View of Soil Microenvironments. *Environmental Science & Technology* 53, 829–837.
640 doi:10.1021/acs.est.8b05245.
- 641 Schmidt, J. E., Kent, A. D., Brisson, V. L., and Gaudin, A. C. M. (2019). Agricultural
642 management and plant selection interactively affect rhizosphere microbial community
643 structure and nitrogen cycling. *Microbiome* 7, 146. doi:10.1186/s40168-019-0756-9.
- 644 Turrini, A., Avio, L., Giovannetti, M., and Agnolucci, M. (2018). Functional
645 Complementarity of Arbuscular Mycorrhizal Fungi and Associated Microbiota: The
646 Challenge of Translational Research. *Front. Plant Sci.* 9.
647 doi:10.3389/fpls.2018.01407.
- 648 Upton, R. N., Bach, E. M., and Hofmockel, K. S. (2019). Spatio-temporal microbial
649 community dynamics within soil aggregates. *Soil Biology and Biochemistry* 132, 58–
650 68. doi:10.1016/j.soilbio.2019.01.016.
- 651 Wilke, A., Bischof, J., Gerlach, W., Glass, E., Harrison, T., Keegan, K. P., et al. (2016). The
652 MG-RAST metagenomics database and portal in 2015. *Nucleic Acids Res* 44, D590–
653 D594. doi:10.1093/nar/gkv1322.
- 654 World reference base for soil resources Available at:
655 <http://www.fao.org/3/w8594e/w8594e00.htm> [Accessed August 3, 2019].
- 656 Wright, S. F., Franke-Snyder, M., Morton, J. B., and Upadhyaya, A. (1996). Time-course
657 study and partial characterization of a protein on hyphae of arbuscular mycorrhizal
658 fungi during active colonization of roots. *Plant Soil* 181, 193–203.
659 doi:10.1007/BF00012053.
- 660 Xu, J., Liu, S., Song, S., Guo, H., Tang, J., Yong, J. W. H., et al. (2018). Arbuscular
661 mycorrhizal fungi influence decomposition and the associated soil microbial
662 community under different soil phosphorus availability. *Soil Biology and Biochemistry*
663 120, 181–190. doi:10.1016/j.soilbio.2018.02.010.
- 664 Yan, Y., Kuramae, E. E., Hollander, M. de, Klinkhamer, P. G. L., and Veen, J. A. van (2017).
665 Functional traits dominate the diversity-related selection of bacterial communities in
666 the rhizosphere. *ISME J* 11, 56–66. doi:10.1038/ismej.2016.108.
- 667 Yao, Q., Li, Z., Song, Y., Wright, S. J., Guo, X., Tringe, S. G., et al. (2018). Community
668 proteogenomics reveals the systemic impact of phosphorus availability on microbial
669 functions in tropical soil. *Nat Ecol Evol* 2, 499–509. doi:10.1038/s41559-017-0463-5.
- 670 Zhang, B., Li, S., Chen, S., Ren, T., Yang, Z., Zhao, H., et al. (2016). Arbuscular mycorrhizal
671 fungi regulate soil respiration and its response to precipitation change in a semiarid
672 steppe. *Scientific Reports* 6, 19990. doi:10.1038/srep19990.
- 673 Zhang, Y., Cui, M., Duan, J., Zhuang, X., Zhuang, G., and Ma, A. (2019). Abundance, rather
674 than composition, of methane-cycling microbes mainly affects methane emissions

675 from different vegetation soils in the Zoige alpine wetland. *MicrobiologyOpen* 8,
676 e00699. doi:10.1002/mbo3.699.

677

678 **Figures Captions**

679

680 **Figure 1** A. Dry shoot biomass of clover inoculated with the AMF *R. irregularis* (A)
681 and the non-inoculated controls (C) (n=10). B. Shoot biomass for the main
682 treatments A, C and including the rotated core control (rC) (n=5). The full
683 comparisons with all replicates are available in Supp. Material 1. C. AMF
684 hyphal length (in m g⁻¹ of soil). D. Hyphal length of other fungi (in m g⁻¹ of
685 soil). E. New aggregates > 2mm (%). F. Water stable aggregates (%). The
686 ANOVA *P*-value results are reported on the bottom of each graph and
687 small letters below the treatment codes, when different, indicate statistical
688 differences by the Tukey posthoc test (*P*<0.05). The gray dots on the box-
689 plots indicate the individual value of each replicate. The dark dot indicates
690 the mean and error bars the standard error.

691

692 **Figure 2** Metabolic functions in soil clustered by the MG-RAST SEED classification
693 accessed by soil metatranscriptomics **(A)** and metaproteomics **(B)**. The
694 sample codes are: static soil core inoculated with the AMF *R. irregularis*
695 (A), non-inoculated static soil core (C), and non-inoculated rotated soil
696 core (rC). For the RNA samples, the prefix **m** indicates the mRNA libraries
697 enriched by rRNA depletion, the other samples without prefix indicate the
698 poly-A selection libraries.

699

700 **Figure 3** The network connectivity of soil metabolic functions (SEED level 1) across
701 treatments for the metatranscriptome (**C.**) and the metaproteome (**D.**). In
702 blue the treatment inoculated with the AMF *R. irregularis* (**A.**), in green the
703 control soil (**C.**) and in salmon the control with rotated soil cores (**rC.**)
704

705 **Figure 4** Changes in the soil microbial community structures based on the taxonomic
706 annotation of the sequences. On top are the general high order taxonomy
707 for the RNA-seq data (**A.**) and for the proteome data (**B.**) (for details on
708 the proteome see Supp. Figure 4). In the middle are the microbial
709 community structures accessed by the redundancy analysis (RDA) based
710 on the RNA-seq for *Bacteria* (**C1.**) and for *Eukaryota* (**D1.**). Below are the
711 phyla relative abundance of *Bacteria* (**C2.**) and *Eukaryota* (**D2.**) across the
712 treatments. The sample codes are: static soil core inoculated with the AMF
713 *R. irregularis* (**A.**), non-inoculated static soil core (**C.**), and non-inoculated
714 rotated soil core (**rC.**). For the RNA samples, the prefix **m** indicate the
715 mixed libraries made using the rRNA depletion.
716

717 **Figure 5** The genes and proteins potentially related with soil aggregation. The panel
718 on top show the z-score of Lpt genes across the samples (**A.**). Below is
719 the quantification of proteins identified in relation to the *R. irregularis*
720 proteome database. The MS intensity signal for Tubulin (Alfa+Beta) (**B1.**),
721 GroeEL/HSP60 (**B2.**) and HSP70 (uniprot U9SYW5) (**B3.**). The sample
722 codes are: static soil core inoculated with the AMF *R. irregularis* (**A.**), non-
723 inoculated static soil core (**C.**), and non-inoculated rotated soil core (**rC.**)
724

725 **Supporting Information**

726

727 **Figure S1** Cumming plots for the classical variables evaluated in the experiment. **A.**

728 Clover dry shoot biomass. **B.** AMF hyphae length (in m.g^{-1} of soil). **C.**

729 Hyphae length of other fungi (in m.g^{-1} of soil). **D.** AMF spores observed

730 during the hyphae length measurements **E.** New aggregates > 2mm (%)

731 **F.** Water stable aggregates (%). The codes are: A, soil inoculated with

732 the AMF *R. irregularis*, C, control soil (static core), and rC, the rotated

733 core soil.

734

735 **Figure S2** Summary of the RNA-seq results. In panel **A.** the read counts across the

736 treatments; in **B.** Effect size and Volcano plot generated by Aldex2

737 showing all the transcripts as dots and in light colors are the transcripts

738 that had statistical significant changes in relation to the rotated core

739 ($P < 0.05$).

740

741 **Figure S3** Proteome data after the ANPELA server processing. A. Heatmap of all the

742 identified proteins according to treatments (ANPELA normalized values).

743 The sample codes are: static soil core inoculated with the AMF *R.*

744 *irregularis* (A), non-inoculated static soil core (C), and non-inoculated

745 rotated soil core (rC). B. A volcano plot showing significantly regulated

746 proteins between the AMF treatments and the rotated core control

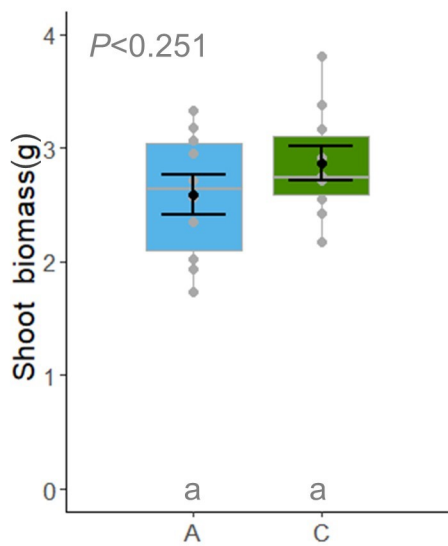
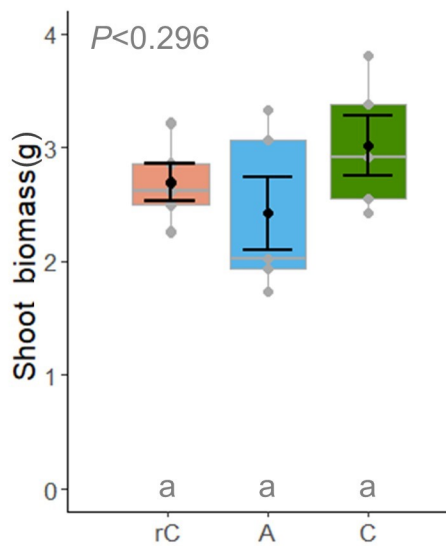
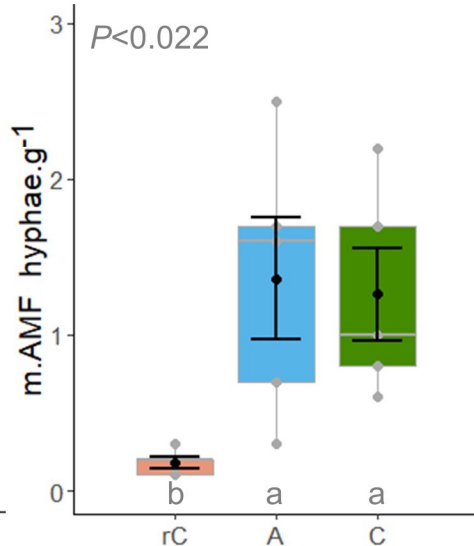
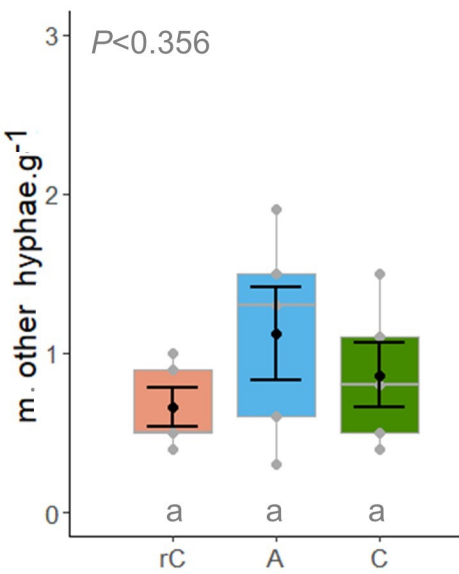
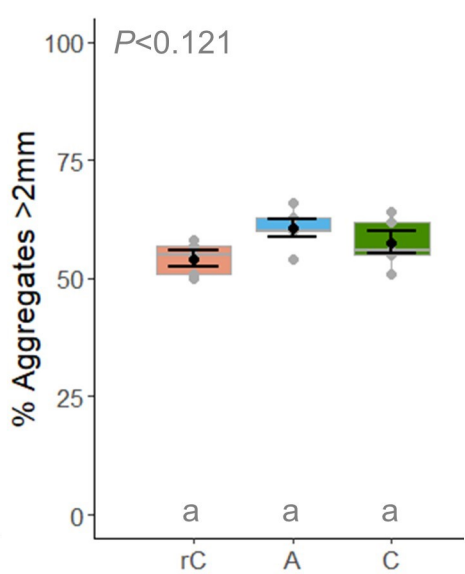
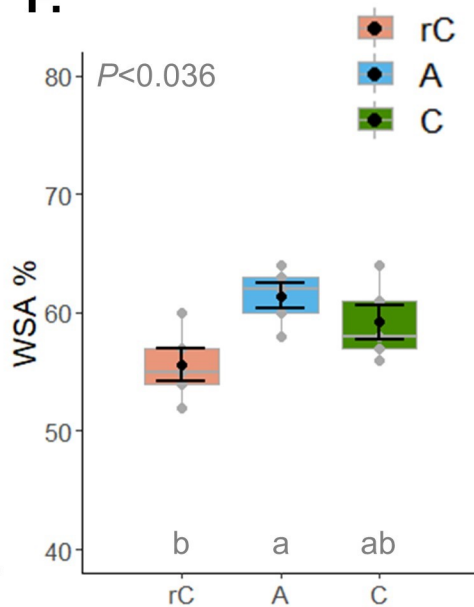
747 ($P < 0.01$).

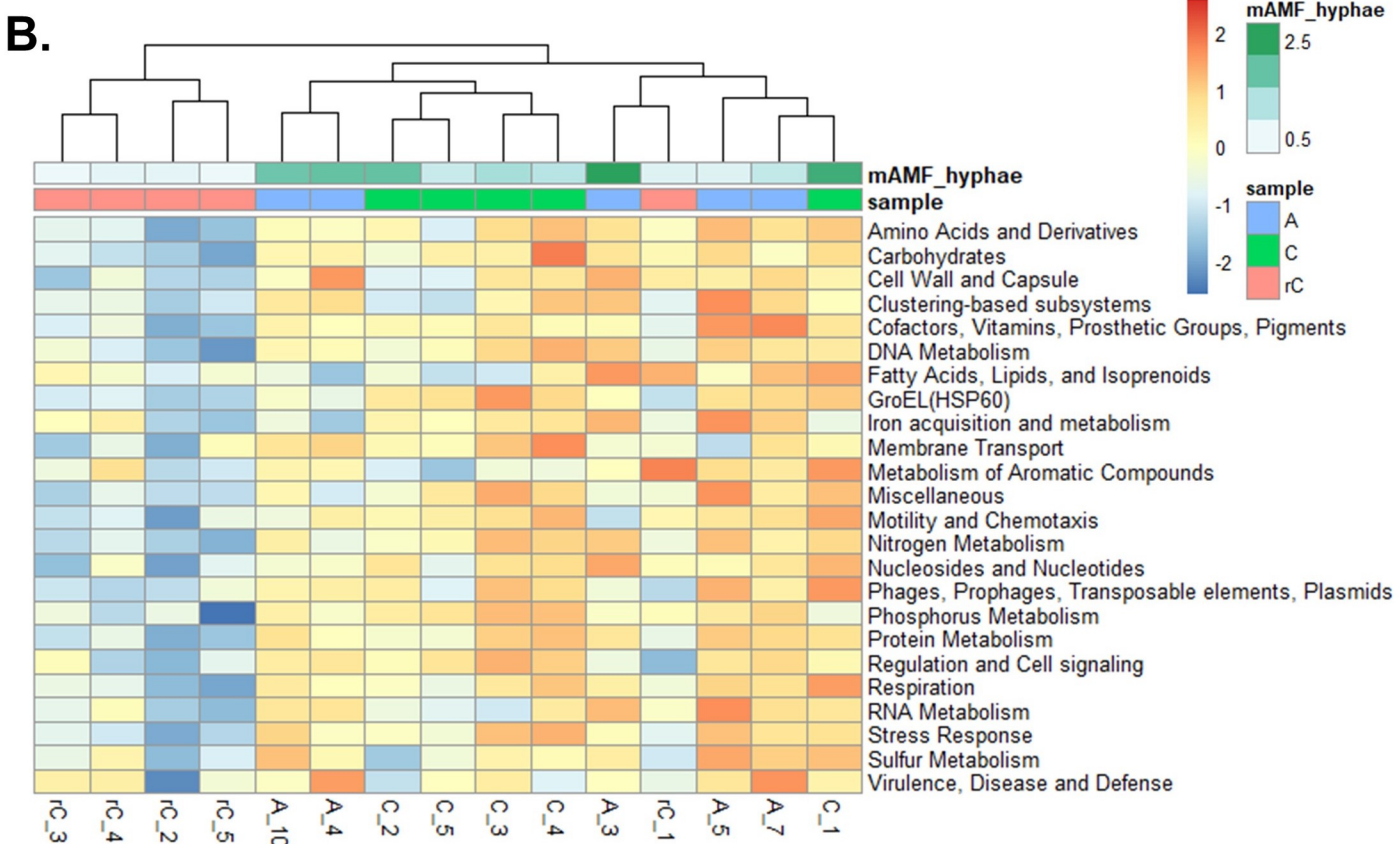
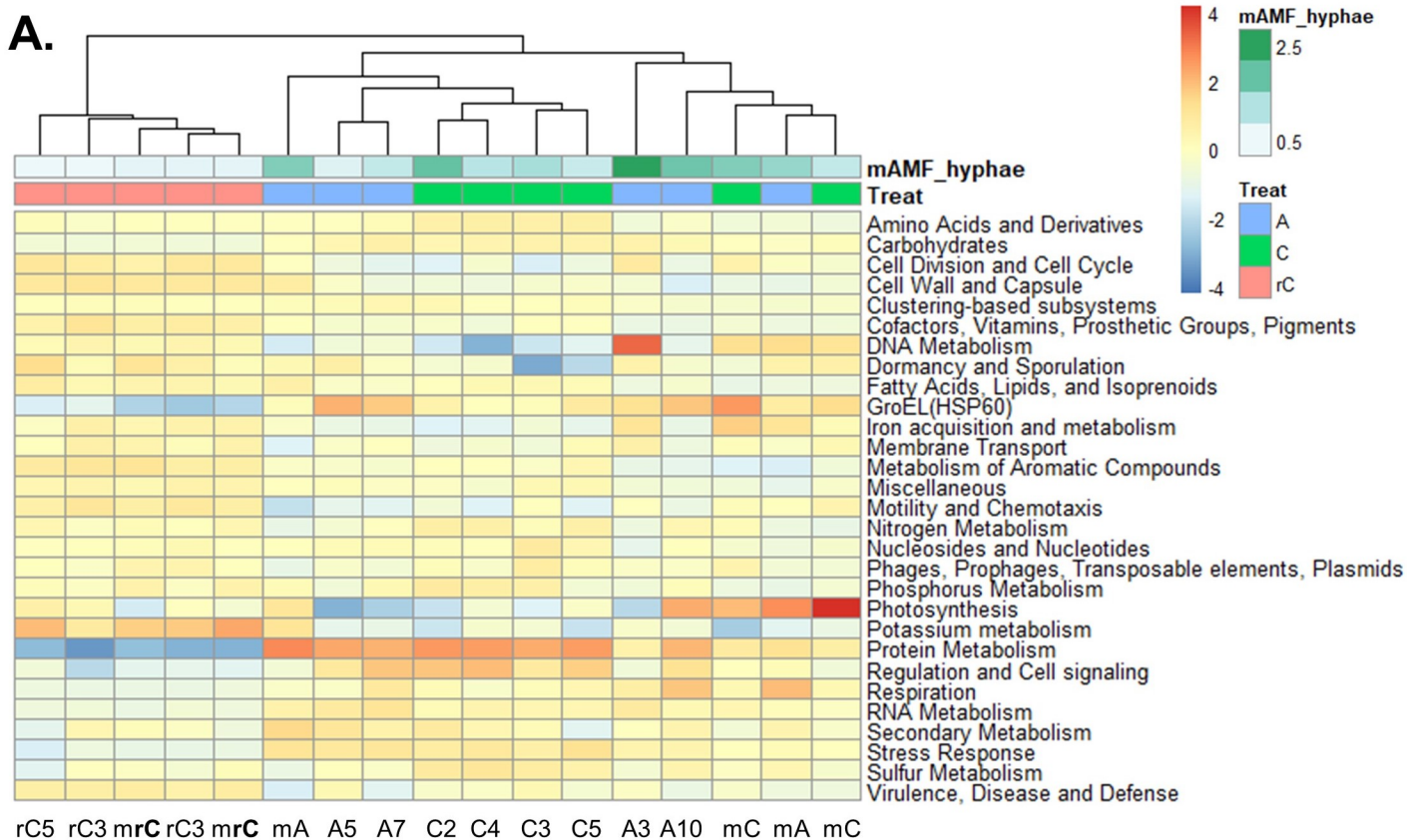
748

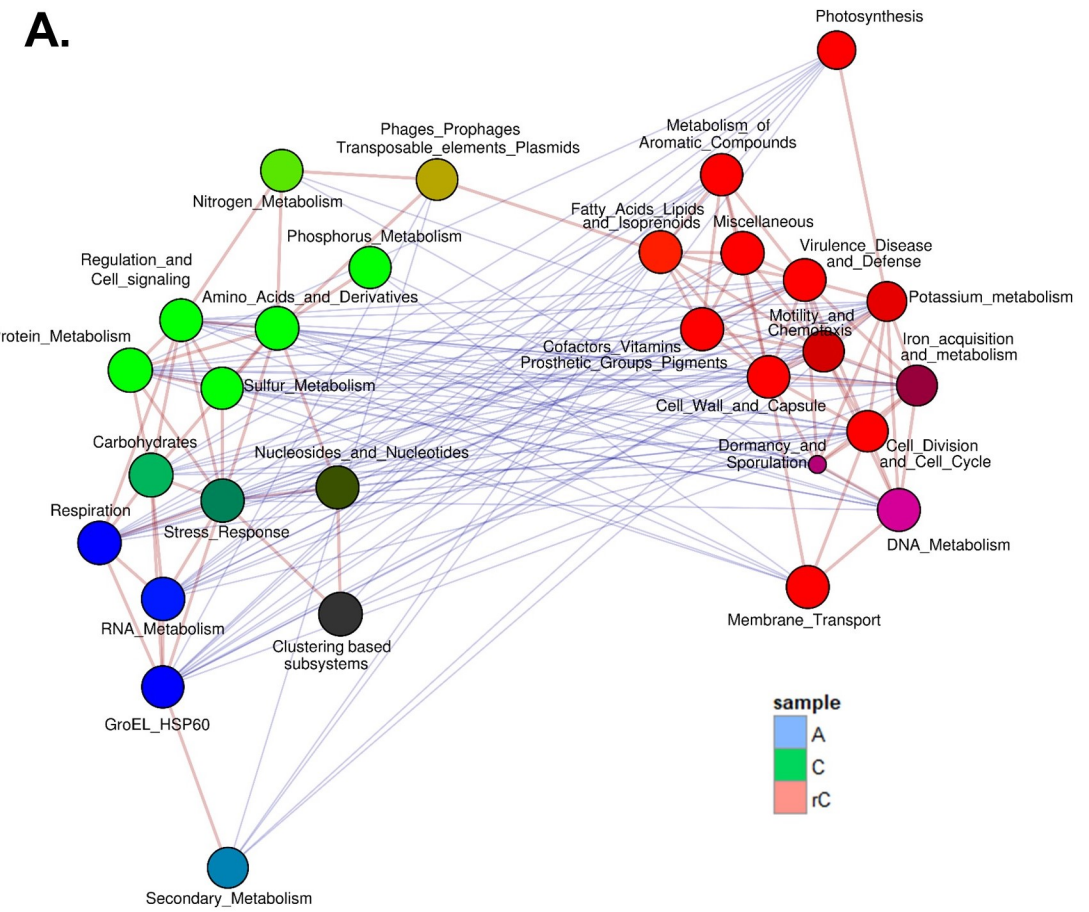
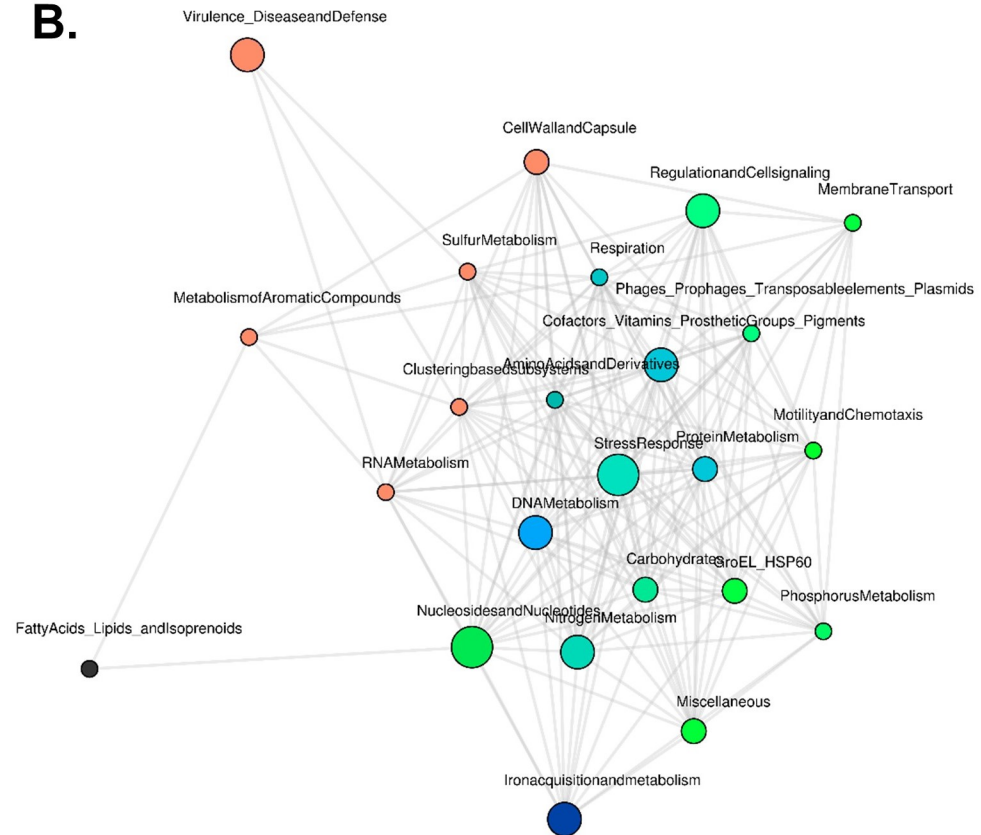
749 **Figure S4** The relative abundance of the all proteins identified by the taxonomic
750 annotation for *Bacteria* (**A.**) and *Eukaryota* (**B.**) across the treatments.
751 The sample codes are: static soil core inoculated with the AMF *R.*
752 *irregularis* (A), non-inoculated static soil core (C), and non-inoculated
753 rotated soil core (rC).

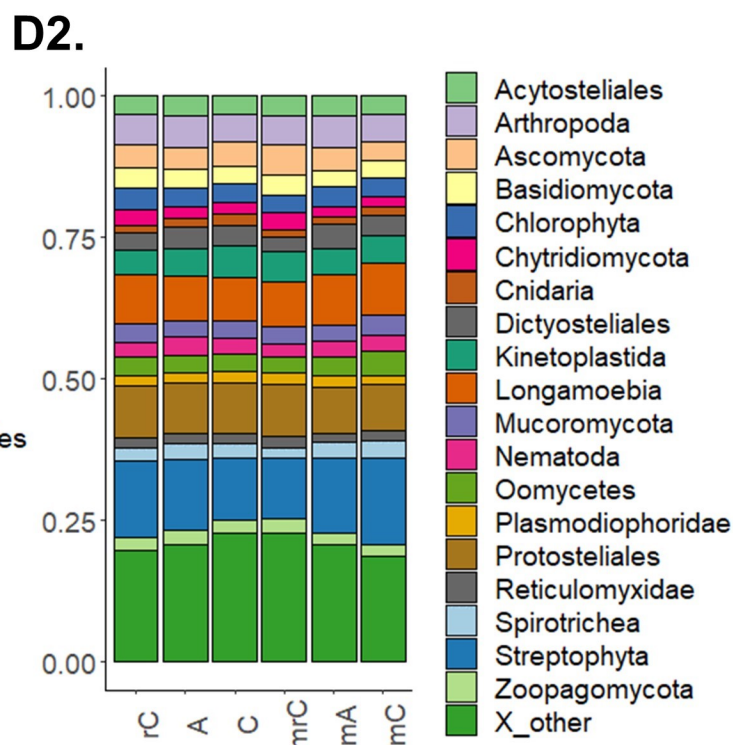
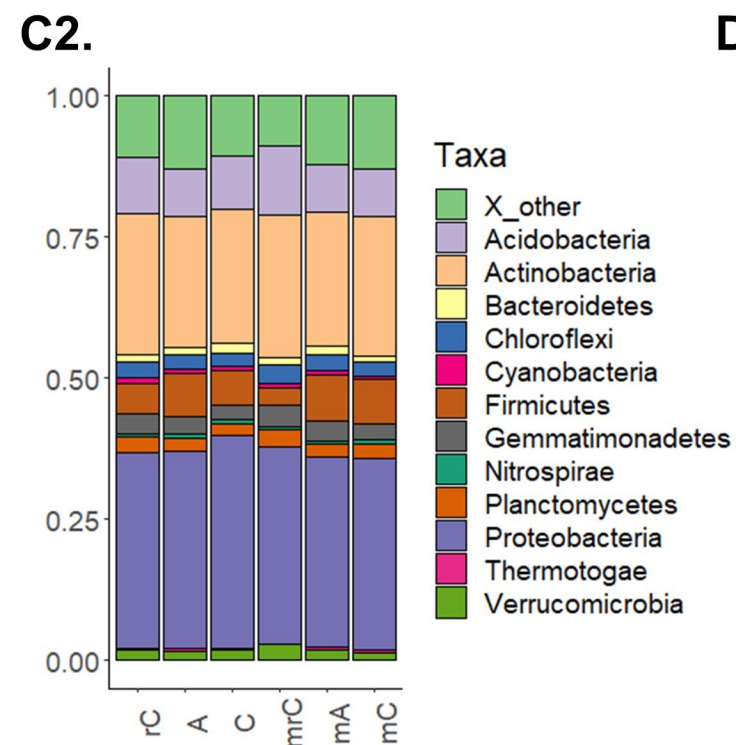
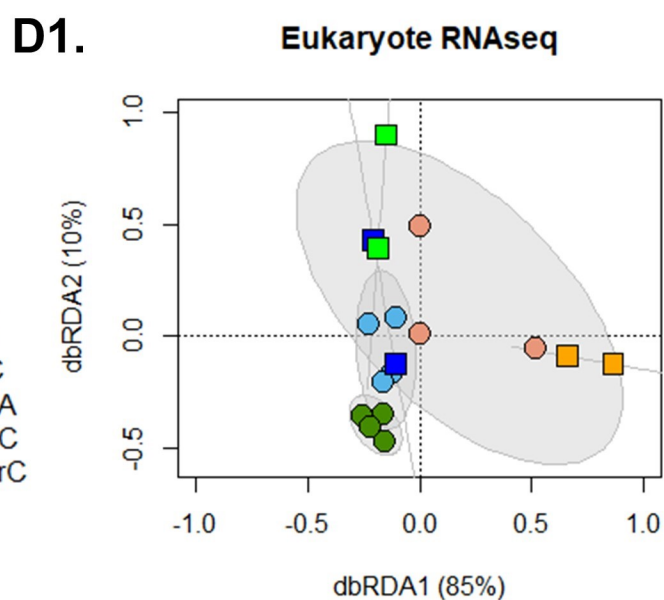
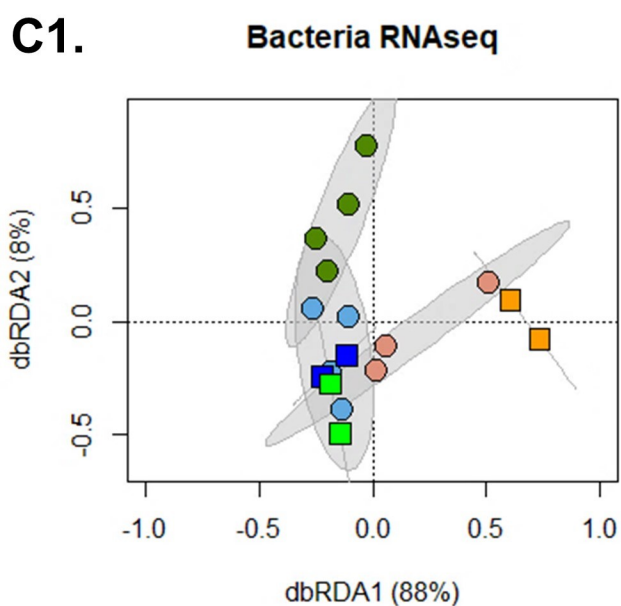
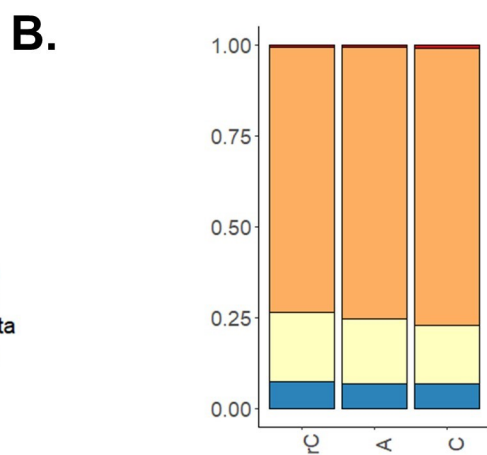
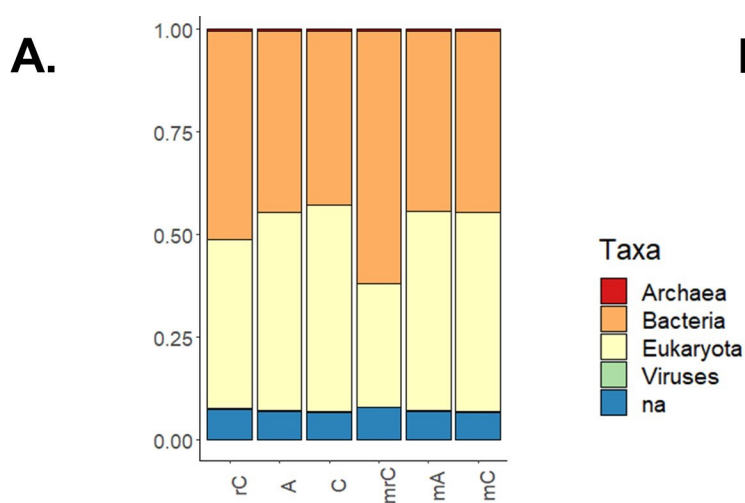
754

755 **Figure S5** The relative abundance of the GroeL/HSP60 reads of the RNAseq based
756 on the high order taxonomy (**A1.**) and according to *Bacteria* (**A2.**) and
757 *Eukaryote* (**A3.**) phyla. On the bottom right is the relative abundance of
758 the GroeL/HSP60 proteins across the proteomes (**B**). The sample codes
759 are: static soil core inoculated with the AMF *R. irregularis* (A), non-
760 inoculated static soil core (C), and non-inoculated rotated soil core (rC).
761 For the RNA samples, the prefix m indicate the mixed libraries made
762 using the rRNA depletion.

A.**B.****C.****D.****E.****F.**

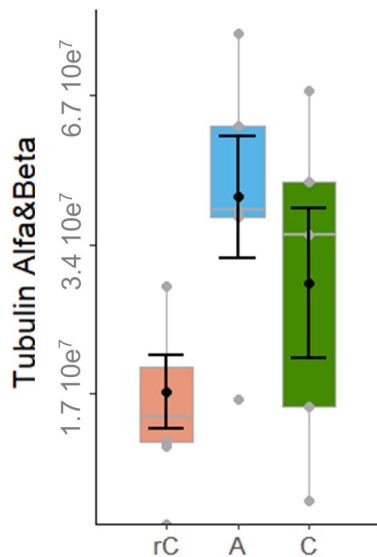
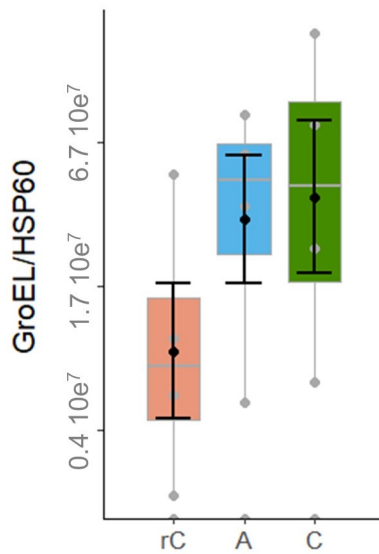


A.**B.**



A.

	rC	A	C	mrC	mA	mC
LptC (Bacteria)	0.6	0.3	0.0	0.8	0.1	0.1
LptF (Bacteria)	0.7	0.1	0.2	0.9	0.1	0.0
LptG (Bacteria)	0.7	0.1	0.1	0.8	0.1	0.1

B1.**B2.****B3.**